Trends in Welding Research: Proceedings of the 6th International Conference
Stan A. David, Tarasankar DebRoy, John C. Lippold,
Herschel B. Smartt, John M. Vitek, editors, p 878-885
DOI: 10.1361/cp2002twr0878

6th International Trends in Welding Research Conference Proceedings, 15-19 April 2002, Pine Mountain, GA, ASM International, 2003

Diffraction Strain Measurements for the Characterization of Residual Stresses in Welds for Gas Turbine Applications

D. Dye, K. T. Conlon
National Research Council of Canada, Chalk River Laboratories,
Chalk River, Ontario K0J 1J0, Canada
R. C. Reed
Dept. of Metals and Materials Engineering, University of British Columbia,
309-6350 Stores Road, Vancouver, B.C. V6T 1Z4, Canada
K. E. James, A. M. Korsunsky
University of Oxford/Rolls-Royce UTC, Dept. of Engineering Science,
Parks Road, Oxford OX1 3PJ, UK

Abstract

Neutron and synchrotron x-ray diffraction strain measurements around gas tungsten arc and electron beam welds are used to characterise the state of residual stress in an aero-engine component and testpieces in wrought nickel-base superalloys. Spatial resolution is typically found to be around 1 mm and typical counting times are around 15 minutes per orientation for neutron diffraction and 10 s for synchrotron x-rays. The effects of intergranular, orientation-dependent strains are discussed and their avoidance in the determination of engineering strain illustrated. Grain size and beam divergence are found to limit the spatial resolution that can be achieved, and this illustrates why in-weld measurements made using these techniques can be unreliable. These effects are explored using case studies in gas tungsten arc, electron beam and low stress low distortion welds in IN718 and C263 and electron-beam welds in a Waspaloy plate and compressor disc assembly.

Introduction

Welding operations are widely used by gas turbine manufacturers for the fabrication of aero-engines, in particular the combustor and compressor assemblies. Considerable care must be taken during welding because of the residual stresses and distortion caused by welding [1, 2]. Distortion, if not properly controlled, can exceed tolerances, generating rework and scrap. Residual stresses are also undesirable because of the effect on component life, and heat treatment is often used, where possible, to reduce the levels of welding-induced residual stress. During the final stages of fabrication heat treatment often becomes impractical or uneconomic because of the differing heat treatments required for dissimilar alloys and because of the assembly size. Therefore it is generally desirable to be able to characterise, and model, such stresses.

Diffraction methods of strain measurement are often attractive because (i) they are non-destructive and (ii) they are 'direct' - that is they give a direct measure of elastic strain and do not require calculation of the stress field from the relaxation observed after hole-drilling or component sectioning. Furthermore, neutron and synchrotron x-ray diffraction allow the measurement of strains many millimetres deep within a material, whereas most other methods can only detect surface or near-surface stresses.

Over the past decade or so, a significant effort has been directed at developing diffraction strain measurement techniques to the point where they can be applied routinely to industrial problems. In particular, the effects of so-called intergranular strains, caused by plastic strain, upon the measured strain field have been characterized in order to allow the measurement of the macroscopic, engineering strain.

In this paper we demonstrate how accounting for these effects in nickel alloys has allowed us to measure the engineering stress state in welds produced by both electron-beam and arc welding, for comparison with process models for welding. We also illustrate how the emerging field of synchrotron x-ray diffraction allows similar results to be achieved much faster than with neutrons, owing to the higher flux present at third-generation x-ray sources such as the ESRF, Grenoble, France. However, this new technique has distinct challenges from neutron diffraction which we illustrate using measurements performed on a test weld in the nickel-base alloy C263 by both neutron and synchrotron x-ray diffraction.

Principle of diffraction strain measurement

The principle of diffraction strain measurement is to equate changes in interatomic spacing to elastic strains. Therefore the change in interplanar spacing of an $\{hkl\}$ plane d^{hkl} is recognised as the strain component i,

$$\varepsilon_i^{hkl} = (d_i^{hkl} - d_0^{hkl})/d_0^{hkl} \tag{1}$$

A diffraction strain measurement is therefore composed of simply measuring d-spacings in directions of interest within the sample. The principal directions are assumed to be aligned with those of the welding path and sample, so the conversion to stress is straightforward,

$$\sigma_i = \frac{E}{1+\nu}\varepsilon_i + \frac{E\nu}{(1+\nu)(1-2\nu)}\Sigma\varepsilon_i \tag{2}$$

where E and ν are the Young's modulus and Poisson's ratio, respectively, σ and ε denote stress and strain and $i = 1, 2, 3$ are the (orthogonal) principal directions. Thus diffraction strain measurements provide a direct measure of the elastic strains experienced by the population of grains in the diffracting condition given by Bragg's Law, $\lambda = 2d_{hkl} \sin\theta$, where λ is the wavelength of the radiation employed and θ is half the diffraction angle.

Effect of elastic and plastic anisotropy

Measurements made on different populations of grains using different diffraction peaks $\{hkl\}$, corresponding to different grain orientations with respect to the measurement axes, usually give different values for the strains measured [3], because of the effects of the elastic and plastic anisotropy found in most metal single crystals.

The effect of elastic anisotropy cannot simply be dealt with through a rotation of the single crystal stiffness matrix to find the stiffness of the single crystal in the $\{hkl\}$ direction, because of strain accommodation between neighbouring grains. However, models such as the inclusion-in-medium approach of Eshelby [4, 5] have been highly successful at predicting the effective average stiffness (the diffraction elastic constants, or DEC's) of $\{hkl\}$-oriented grains as measured in tensile tests and simple programs are available to make such predictions. Therefore elastic anisotropy is usually dealt with using either measured diffraction elastic constants (DEC's) in Equation 2 or, for single phase materials, DEC's calculated from the single crystal elastic constants [6, 7].

Plastic anisotropy results in the flow of grains in weaker orientations at lower total loads than those in stronger orientations, illustrated by Schmid's law - that the failure stress σ_y of a single crystal in tension is given by $\sigma_y = \tau_c / m_s$, where τ_c is the critical resolved shear stress for dislocation motion and m_s is the orientation-dependent Schmid factor. During a simple tensile test, in the limit of perfect plasticity, the grains that have already plastified experience no accumulation of load beyond their elastic limit and additional load is transferred to grains in stronger orientations, as shown in Figure 1. On unloading after plastic straining, if there is no reverse yielding, the different amounts of plastic strain experienced by grains in different orientations results in the observation of residual intergranular strains between grains in different orientations, $\Delta\varepsilon_{hkl}$.

These intergranular stresses caused by plastic deformation are inconvenient, because if they are superposed with an external stress field then a diffraction strain measurement cannot be directly used to determine the macroscopic stress. Therefore much research has concentrated on the identification of $\{hkl\}$ orientations [8, 9, 10, 11], or combinations of orientations, which do not accumulate significant microstrains and therefore are suitable for measurement of the macroscopic strain field. In, nickel-base alloys it has been found that the {111} and {311} reflections do not accumulate significant microstrains during tensile tests and are therefore appropriate for the determination of elastic strain [7, 12, 13].

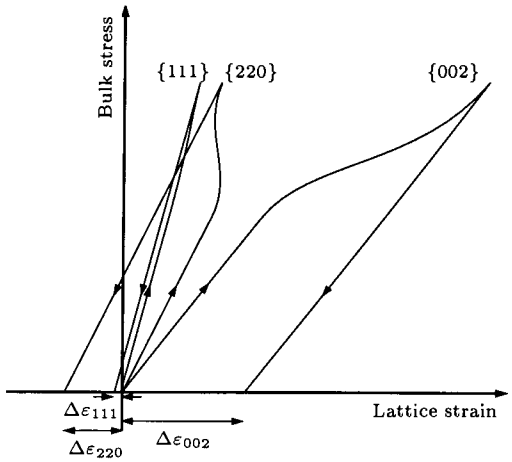

Figure 1: Illustration of lattice strain response in the loading direction during a tensile test for grains orientated with {002}, {111} and {220} lattice planes perpendicular to the loading direction. The behaviour shown is representative of nickel alloys and of austenitic steels.

Weld Manufacture and Characterization

An 80 mm long autogenous bead-on-plate weld was placed on a 100 × 50 × 2 mm rectilinear testpiece of the nickel-base superalloy C263, using square-wave d.c. gas tungsten arc welding (GTAW) using a nominal welding power of 580 W and a welding speed of 1.6 mm s^{-1}, resulting in a heat input of 360 J mm^{-1}. C263 is primarily composed of a matrix phase γ-Ni, with precipitates of γ'-Ni_3Al. The workpiece was insulated from the welding jig using graphite plates and was unconstrained in order to simplify the problem for finite element modelling [14]. The material used was as-received commercial sheet in the solution heat-treated condition, supplied by Haynes Int'l (Manchester, U.K.).

A further 180 mm long weld was manufactured under the same welding conditions [15], placed centrally on a 200 × 100 × 2 mm rectilinear testpiece of solution heat-treated IN718, also supplied by Haynes Int'l. IN718 is also a γ'-strengthened superalloy, but has additional precipitates of γ''-Ni_3Nb, which is the major strengthening phase. In addition, a component analogue was constructed for the purpose of mechanical testing, composed of a membrane of 1.75 mm thick solution heat-treated sheet IN718 welded between two circular 14 mm thick IN718 forgings. Electron beam-welding was used to manufacture the assembly, at a welding speed of up to 12.6 mm s^{-1}. Further details are given in [16]. Electron-beam welds were manufactured in a 200 × 50 × 4.3 mm plate of Waspaloy [17] and in an aero-engine compressor disc assembly with the same joint thickness and welding conditions [18]. The stress in the assembly was measured after stress-relief heat treatment.

Neutron Diffraction Measurements

Neutron diffraction strain measurements using the {111} reflection were made on the C263 test weld using the D1A diffractometer at the ILL, Grenoble, France. A wavelength of

sample	instrument	method	E (GPa)	ν	σ_y (MPa)	E_{111} (GPa)	ν_{111}	d_0 (Å)
C263 sheet	D1A	neutron	223	0.29	400	261	0.25	3.5877
	ID11	synchrotron						3.5894
IN718 sheet	ENGIN	neutron	204	0.30	300	246	0.26	3.6023
IN718 disc	ID11	synchrotron	204	0.30	450	246	0.26	
Waspaloy plate	L3	neutron	199	0.3	900	257	0.25	3.5798
Waspaloy disc	L3	neutron						

Table 1: Material Young's Modulus E, Poisson's ratio ν and yield stress σ_y, diffraction elastic constants, and strain-free lattice parameter used in each of the diffraction strain measurements.

2.994 Å was employed. Measurements were made in the longitudinal, transverse and through-thickness directions. The gauge volume used was $1 \times 1 \times 1$ mm for the measurements of longitudinal strain and $1 \times 1 \times 10$ mm for the transverse and through-thickness, making the assumption that these components do not vary parallel to the weld path. In order to establish the strain free lattice parameter d_0, $2 \times 2 \times 50$ mm samples were obtained from a nominally identical weld. The measured lattice strains were converted to stress using diffraction elastic constants calculated from a volume fraction weighted average of the single crystal elastic constants for the γ and γ' phases using Hauk's algorithm [6], scaled to give the correct bulk elastic properties. This approach has been shown to possess an uncertainty of around 8% [12]. The material properties used are given in Table 1.

Measurements in the IN718 plate were made with the ENGIN diffractometer at ISIS, Oxfordshire, UK [15]. Measurements were made in the longitudinal, transverse and through-thickness directions. ISIS is a spallation neutron source, allowing the collection of the entire diffraction pattern at a diffraction angle, 2θ, equal to 90°. Rietveld refinement was used to determine a single lattice parameter, a, for all the peaks, an approach which has been demonstrated to give an accurate measure of the mechanical elastic strain in cubic materials [19].

Measurements in the Waspaloy electron-beam welded compressor disc and test plate were performed using the L3 diffractometer at the National Research Council, Chalk River Laboratories, Ontario, Canada [17, 18]. The {111} reflection was used to determine the strain in all three of the assumed principal directions. For the disc, slits were used on the incident side to define the diffracting volume, of size 20 mm in the circumferential and radial directions and 1 mm in the axial direction but it was not possible to place a slit on the scattered side sufficiently close to define a gauge volume. The angular divergence was limited using Soller slits to 0.4 ° in both the incident and diffracted beams. With this configuration, step scanning of $\theta - 2\theta$ was required to avoid the problems of an artificial peak shift due to the gauge volume being defined by the sample. Such a $\theta - 2\theta$ scan in reciprocal space guarantees that a true lattice parameter measurement is made.

Synchrotron Diffraction Measurements

Synchrotron diffraction measurements were performed on the ID11 beamline using a KUMA single crystal diffractometer on the same C263 testpiece, using an incident x-ray wavelength of 0.2529 Å, equivalent to an energy of 49.15 keV. Incident slits were used to define the diffracting volume, which was 0.5 mm in the transverse direction of the weld and 1 mm in the longitudinal direction of the plate. Measurements were made in the longitudinal and transverse directions (plane stress assumed) using the {111} peak, at a diffraction angle of approximately 3.49 °. A further set of measurements were performed in the web of the IN718 component analogue using a Frelon CCD image plate detector [16], which was used to capture the entire diffraction ring. The ring diameter was then measured in the central 10 ° segment corresponding to each of the longitudinal and transverse directions. These measurements required less than 10 s per measurement location, including the time required for stage motion and data acquisition. For comparison, the neutron measurements require around 15 minutes per orientation, depending on the instrument and sampling volume.

Results

C263 test weld

A comparison of the longitudinal and transverse {111} lattice strains measured by both neutron and synchrotron diffraction is shown in Figure 2(a) and (b). The weld width was approximately 5.8 mm, and the strong weld texture and large grain size inhibited measurements within the weld zone. The measured longitudinal strain is constant in the heat-affected zone up to a distance of 5.5 mm from the weld centreline, at around 1600 microstrain ($\mu\varepsilon$), and then declines at $275 \pm 25\,\mu\varepsilon\,\mathrm{mm}^{-1}$ to a constant strain in the far field of $-1250 \pm 250\,\mu\varepsilon$ in the far field 15 mm from the weld centreline. The rather large uncertainty occurs because of a systematic difference between the two measurements in the far field which is not present in the heat-affected zone. Both measurements account for a 400×10^{-6} variation in the measured strain free lattice parameter d_0 across the welded testpiece, which is consistent in form between the two techniques. The statistical uncertainty from the peak fits is not shown, but is negligible in the case of the synchrotron measurements and are around $50\,\mu\varepsilon$ in the neutron measurements. However, there are additional sources of uncertainty, primarily from the diffraction elastic constants, microstrain accumulation and grain sampling.

The transverse measurements of {111} lattice strain made by neutron diffraction show a consistent but small increase in

strain from the heat-affected zone to the base metal of around 400 $\mu\varepsilon$. However, the synchrotron measurements show much greater scatter with an apparent standard deviation of around 200 $\mu\varepsilon$. It should be pointed out that once this uncertainty is taken into account, the two sets of measurements are broadly in agreement and that an uncertainty of this magnitude, while undesirable, is only noticeable because the strain variation across the weld is so small - in a tensile test 200 $\mu\varepsilon$ corresponds to approximately 40 MPa in this alloy. In general, measurements of transverse strain show greater scatter than for the longitudinal strain [3]. This is because grains in a given orientation in the transverse direction posses a range of orientations in the longitudinal direction and therefore, because of their differing elastic response in the longitudinal direction, will have a range of Poisson contractions due to the applied longitudinal strain. This argument implies that a strain measurement along a secondary axis of stress must sample a greater number of grains in order to arrive at a meaningful average, and that the measured peak width will be greater than for measurements made in the primary (*i.e.* longitudinal) stress direction.

The deduced longitudinal stresses compare well to a finite element model for this weld [14], Figure 2(c), and again are consistent between the two sets of measurements, *i.e.* the deduced primary stresses are insensitive to the variations in measured transverse strain in the synchrotron measurements. The peak longitudinal stress of 450±25 MPa occurs adjacent to the weld in the heat-affected zone and extends to a distance of 5 mm from the weld centreline, after which the stress declines to approximately -300 ± 100 MPa and is constant in the far field 14 mm from the weld centreline. The measurements indicate that the model slightly under-predicts the width of the tensile region in the weld, but that the magnitude and form of the predicted stress variation is correct. The under-prediction of the tensile zone width by model, which was calibrated for a test weld in IN718, is probably due to an under-estimate of the amount of heat deposited by the welding process [14, 20]. As with the longitudinal strain, the measurements appear to give systematically different results in the far field. The transverse and through-thickness stresses found by neutron diffraction are both small and slightly compressive, between 0 and -75 MPa throughout the heat-affected zone [14].

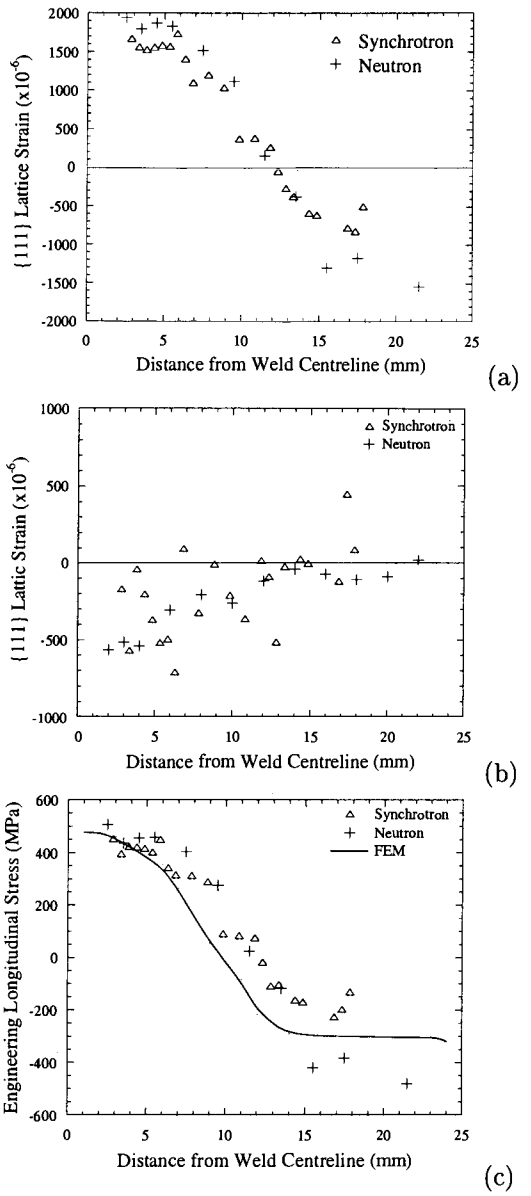

Figure 2: Strain and stress state measured by synchrotron x-ray and neutron diffraction in the C263 plate, and the longitudinal stress predicted by a finite element model.

IN718 test plate and component analogue

Neutron diffraction measurements were made in several locations along the length of the weld in the IN718 test plate, Figures 3 and 4. In addition, incremental hole-drilling using a 1.6 mm hole diameter was carried out at three locations in the heat-affected zone according to ASTM standard E-837-89 [21]. The measurements indicate that the longitudinal stress at mid-length of the plate was approximately constant between the edge of the fusion zone and 8 mm from the weld and of value 255 ± 25 MPa. The stress then decreases to a minimum of -150 ± 20 MPa at a distance of 16 mm from the weld centreline. The longitudinal stress then increases to approximately zero in the far field away from the weld. The stress profile is mostly unchanged, to within 50 MPa, along the central 140 mm of the 180 mm long weld bead.

The transverse stress is compressive immediately adjacent to the weld at around -120 MPa, and increases to approximately zero in the far field over the region between 8 and 16 mm from the weld centreline. The longitudinal and transverse stresses measured by hole drilling are in broad agreement with those measured by neutron diffraction. The measured through-thickness stresses in the weld mid-depth are significant, at up to -150 MPa in the region immediately adjacent to the weld. However, they rapidly decrease to zero in the heat-affected zone 16 mm away from the weld centre.

This indicates that near the weld the through-thickness temperature distribution is significant enough to cause non-uniform yielding, giving rise to through-thickness stresses.

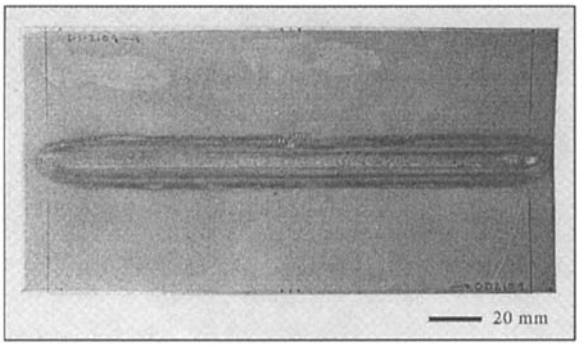

Figure 3: Top view of the as-welded IN718 plate, showing the weld location.

This illustrates that the assumption of plane stress may not be adequate, even in conventional GTAW welding in thin sheets. The hole-drilling and laboratory x-ray techniques are incapable of detecting a through-thickness distribution of stress. The multiple measurements performed on this sample also give an approximate idea of the scatter observed in repeated measurements, which is usually much larger than can be attributed to the fitting uncertainty of the diffraction peak. It is likely that this is at least partially due to the grain sampling effects discussed earlier in relation to the synchrotron measurements in the transverse direction of the C263 weld.

The as-welded IN718 component analogue is shown in Figure 5 and the estimated residual stresses along the 0 ° scan line are shown along with the predictions of a finite element model in Figure 6. No d_0 measurement was made, so the value of d_0 used has been chosen to fit the finite element model. However, the hoop stress profile predicted by the model is in good agreement in both form and magnitude with the predictions made by the model. These are that the outer web is in a state of compression, and that the web is held in tension at around $350 - 400$ MPa between the two welds which are themselves in tension of up to 700 MPa. This is remarkable, since the yield stress of the parent sheet is only 450 MPa. However, the model and measurements also indicate that the radial stress in the web is around $500 - 600$ MPa, and therefore that the web is held in biaxial tension with a significant hydrostatic stress. The stress gradients at the inner and outer edges of the web adjacent to the welds are also in good agreement.

However, several features remain; the measurements indicate that the radial stress increases significantly in the welds, which is not predicted by the model. The model implemented here uses a heat source description optimised for GTAW welding and does not simulate the extremely narrow weld bead and heat source found in electron beam welding. This might be expected to lead to heating over a narrower zone and therefore to a greater concentration of deformation in the weld region, which would explain the discrepancy. Finally, the measurements shown do not provide a stress balance across the segment. It is felt that this is because the balancing region of compressive stress is found in the outer forging, which have much greater cross-sectional area than the sheet composing

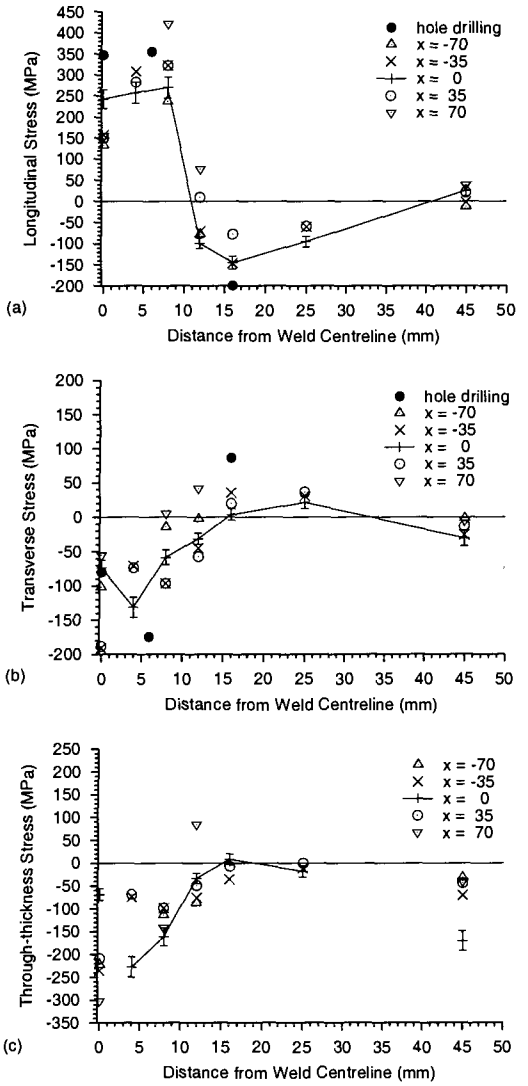

Figure 4: Rietveld-refined stresses in the as-welded IN718 plate, and their comparison to hole-drilling data. The mid-length of the weld corresponds to $x = 0$, with the positive x direction coincident with the welding direction. Hole drilling measurements were made at the weld mid-length, $x = 0$.

the web. This stress pattern arises because of the compression produced on heating around each weld due to constrained thermal expansion. In a rectilinear testpiece this compression is alleviated in the transverse direction by lateral shrinkage of the plate, but in this testpiece the radial stress cannot be relieved in a similar fashion because of the constraint of the forgings, and so a tensile stress is found instead.

The measured d-spacing profiles were found to vary in magnitude but not form or variation between scans along different radii of the plate. It is suggested that this was because the assembly was tilted in the diffractometer. Because the centre of the diffracting volume is defined by the sample and not by slits in the configuration, this would result in an apparent change in scattering angle which would normally interpreted

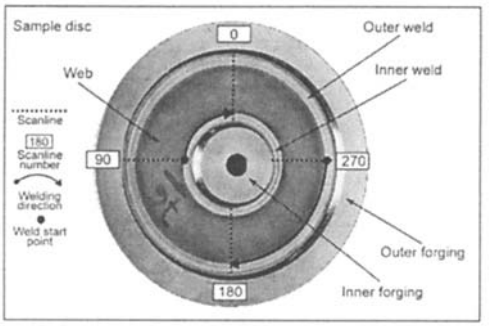

Figure 5: As-welded IN718 component analogue composed of sheet IN718 welded between two circular forgings.

as a d-spacing change and therefore to a strain.

Waspaloy test plate and compressor disc

The measured state of residual stress in the electron-beam welded Waspaloy testpiece are shown in Figure 7, along with surface measurements made by laboratory x-ray diffraction using the $\sin^2\psi$ method and hole drilling measurements. The measurements are in excellent agreement for the longitudinal and transverse residual stress. Compared to the IN718 and C263 welds the peak longitudinal stress is much higher, because the material was welded in the fully heat-treated condition and because the heat affected zone is much smaller. The peak longitudinal stress is around 1000 MPa immediately adjacent to the fusion zone. This stress decreases rapidly over the next 5 mm, reaching a compressive stress of -200 MPa 7 mm from the centreline, which is then maintained to the edge of the plate.

In comparison, the transverse stress is constant across the entire plate and is approximately zero or slightly compressive. For the neutron measurements the through-thickness strain profile was also determined, but the through-thickness stresses were close to zero and hence are not shown. Measurements within the weld region were not attempted using diffraction because of the large grain size and texture present. The greater thickness of this testpiece made orientation of the specimen on the diffractometer simpler than with sheet materials because the distortions in the welded sample were minimal and because the gauge volume could be reliably buried within the sample. Overall, the consistency of the measurements made on this weld indicate the reliability of all three strain measurement techniques when performed carefully on a well-prepared sample.

The electron-beam welded and postweld heat-treated compressor disc assembly is shown in Figure 8. A section of the joint configuration is shown in Figure 9, and measurements were made in the axial, hoop and radial directions across the 20 mm wide section containing the weld between the two sealing fins, at the mid-depth of the joint thickness. The resulting stresses are shown in Figure 10, where for the radial and hoop strain the uncertainty used was the Gaussian fitting uncertainty and for the axial strain the uncertainty applied was the standard deviation of measurements made at 1/3 and 2/3 of

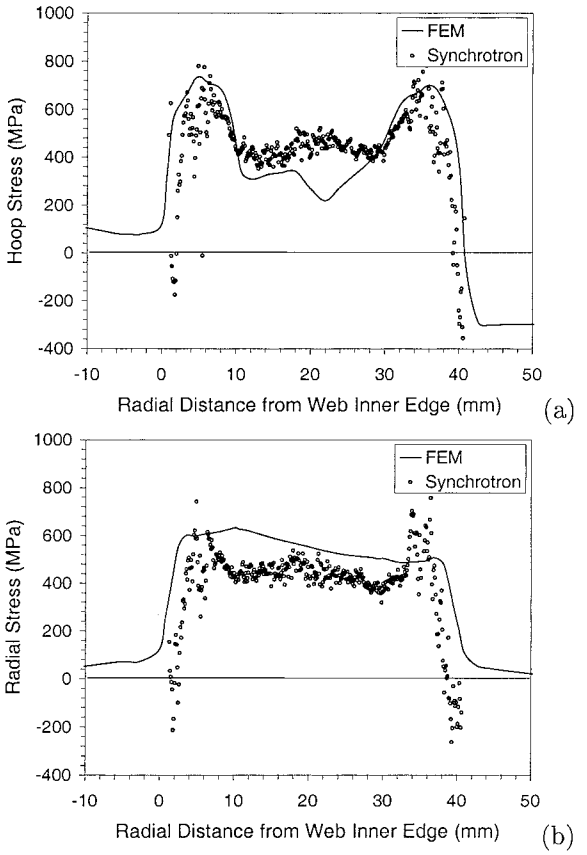

Figure 6: Measured strain profile and finite element model prediction of stresses in the IN718 component analogue.

the wall thickness. Therefore the axial measurements appear to have a larger uncertainty, probably because of a through-thickness variation in strain which is averaged by the other two measurements.

It is observed that the peak longitudinal stress is approximately 400 MPa in the hoop direction, and that the longitudinal stress drops rapidly between 2 and 5 mm from the weld centreline to a compressive stress of between -100 and -200 MPa in the heat-affected zone. The longitudinal stress then rises slightly towards zero with distance from the weld. The radial stresses are much smaller and are generally compressive, in the range of 0 to -100 MPa. The axial stress shows a similar profile, but appears to be asymmetric. It is thought that this is due to the asymmetry of the joint (Figure 9). Once the effect of the postweld heat treatment is accounted for, these measured strains are consistent in pattern with those measured in the as-welded condition above, and in fact show good agreement with those measured in a similar plate after postweld heat-treatment [18].

Discussion

Effect of sample positioning and number of diffracting grains in synchrotron measurements

When performing neutron diffraction strain measurements, it is usual to use a wavelength such that $2\theta \sim 90°$, so that the

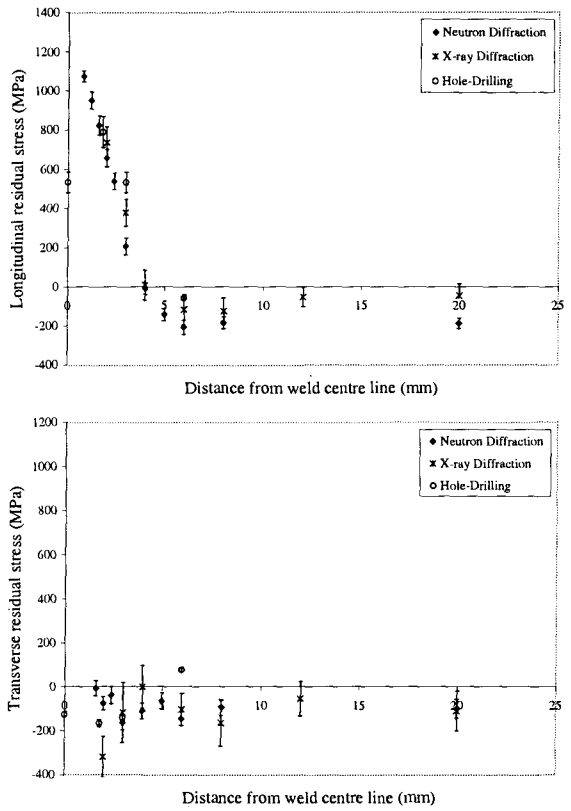

Figure 7: Measured longitudinal and transverse residual stresses in the 4.3 mm thick Waspaloy plate. Comparison is made with measurements made by laboratory x-ray diffraction and hole drilling.

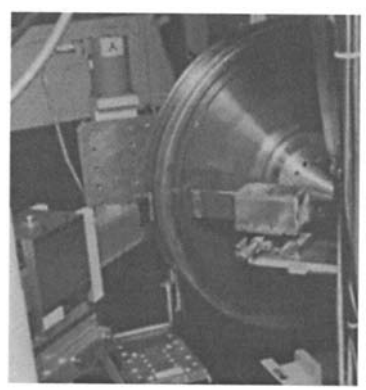

Figure 8: Photograph of the welded compressor disc assembly orientated for measurement of the axial strains and mounted on the L3 diffractometer at Chalk River.

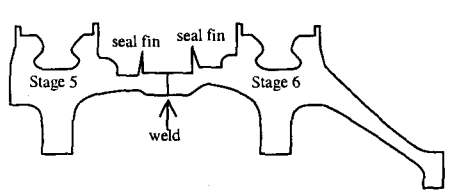

Figure 9: Illustration of the design of the weld of the 5^{th} and 6^{th} stage discs from a Trent 800 high-pressure compressor.

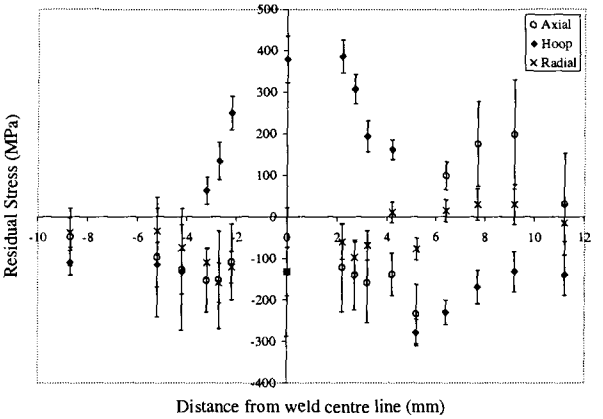

Figure 10: Residual stresses measured across the weld in the steady-state region.

sampling volume is approximately cubic and can easily be defined using slits. However, in order to achieve a sample penetration of several millimetres using synchrotron x-rays it is necessary to use very much shorter wavelengths so that the diffraction angle 2θ is typically less than 12°. This means that defining the diffracting volume using a slit on the scattered side is in practice rather difficult, and therefore that the sample defines the diffracting volume in the through-thickness direction. The determination of the diffraction angle from the ring diameter which is actually measured then requires accurate knowledge of the sample-to-detector distance L. The uncertainty in sample position ΔL therefore results in an uncertainty in the measured strains of magnitude $\Delta L/L$ [16]. Using typical values for $L = 600\,\text{mm}$ and $\Delta L = 0.1\,\text{mm}$ then the uncertainty in the measured strains from this effect will be $170\,\mu\varepsilon$. Two approaches are proposed which would mitigate this problem, (i) to attach a reference material of known d-spacing to the sample for use as a reference, or (ii) to translate the detector and perform two sets of measurements at different distances L, and then to find the corrected diffraction angle from the change in ring diameter.

Another effect which must be considered when using diffraction strain measurement to measure engineering stress is that a significant number of grains must be sampled because the strain in any single grain will be affected by the orientation-dependent elastic and plastic strain in its neighbours. Estimates from the requirements for macroscopic mechanical tests indicates that the number of grains sampled should be at least 30-100 [22]. Because the diffraction condition only specifies the orientation of one axis of the grains, measuring secondary strains such as the transverse strain in a plate weld would require sampling over an even greater number of grains. This effect places a lower limit on the sampling volume that can be used. An interacting effect is that the number of grains sampled is dependent on the beam divergence. In particular, the x-ray synchrotron beams that are currently available have very low divergence compared to those typical for neutron beams, as given by the typical diffraction peak width, w_p, shown in Table 2.

quantity	ND	SXD
V (mm^3)	$5 \times 1.5 \times 1.5$	$0.5 \times 1 \times 2$
w_p,w_i (°)	0.6, 0.4	0.03, 0.4
h (°)	5.2	20
m	8	8
D (μm)	50	50
V/D^3	90,000	8,000
$hwm/4\pi$ ($\times 10^{-3}$)	0.68	1.56
N	60	12

Table 2: Typical parameters for the calculation of the number of diffracting grains in a wrought nickel-base superalloy using neutron (ND) and synchrotron x-ray (SXD) diffraction, using the {111} reflection.

The proportion of grains in the diffraction condition in the sampling volume can be estimated from the effective peak width, w (full width half-maximum), the azimuthal angle of the Debye-Scherrer cone sampled, h, and the multiplicity, m, of the peak. Therefore the number of grains sampled by the diffraction probe N for a given grain size D and gauge volume V can be calculated, Equation 3.

$$N = \frac{V}{D^3}\frac{hwm}{4\pi} \tag{3}$$

If the peak width is much less than the mosaicity w_i, then it is appropriate to combine this with the measured peak width, to give $w = \sqrt{w_p + w_i}$. However, only the portion of these grains in the diffracting condition will be probed by the diffraction technique. Typical values for the measurements presented here are given in Table 2, which indicates that the synchrotron diffraction measurements presented here sample fewer grains than is normal in a neutron diffraction strain measurement. This problem can be mitigated in at least three ways, (i) by performing measurements in several locations with the same stress, *i.e.* at several distances along the weld, and averaging the results, (ii) by synthesizing the strains estimated from several peaks, accounting for the effects of elastic and plastic anisotropy, and (iii) by rocking the sample slightly in θ, making measurements at several angles close to the measurement axes and sampling grains in a greater variety of orientations.

Summary and Conclusions

Neutron and synchrotron x-ray diffraction measurements of stresses in electron beam and gas tungsten arc nickel-base superalloy welds have been presented. These indicate that if the sample strain-free lattice parameter and microstrain behaviour is known then in a fine-grained material measurements of stress can be made with high precision and repeatability using the neutron diffraction technique, even in component-scale specimens.

The neutron diffraction measurements presented in the Waspaloy and IN718 plates agree well with measurements made by laboratory x-ray diffraction and incremental hole drilling and with the predictions of finite element models, lending further confidence to the use of this technique.

The two synchrotron x-ray diffraction measurements presented indicate that reliable measurements can be made very rapidly using this method in thin sheets, but that the effects of sample positioning on the measured diffraction angle need to be accounted for more carefully than with neutron measurements, and that the small divergence of the radiation employed means that additional measures may be desirable to increase the number of grains contributing to the strain measurement.

Acknowledgements

This work was largely carried out in the Universities of Cambridge and Oxford, and was supported by Rolls-Royce, EPSRC, MOD and DTI(CARAD), *via* DERA. We would like to thank Drs. Howard Stone and Tom Holden for their kind permission to present the measurements on Waspaloy in this paper. We would like to acknowledge the work presented here of our collaborators Martin Jensen and Dr. Mark Roberts. Useful conversations with Drs. John Root and Ron Rogge are also acknowledged.

References

[1] *Metals Handbook: Welding, Brazing and Soldering*, Volume 6, p609–646. ASM Int'l, OH, USA, 9th edition (1983).
[2] J. Lancaster. *Handbook of Structural Welding.* Abington Publishing, Cambridge, UK (1992).
[3] D. Dye, H.J. Stone, and R.C. Reed. *Current Opinion in Solid State and Materials Science*, 5, 31–37 (2001).
[4] J.D. Eshelby. *Proceedings of the Royal Society of London A*, 241, 376–396 (1957).
[5] H. Behnken and V. Hauk. *Zeitschrift für Metallkunde*, 77(9), 621–626 (1986).
[6] V. Hauk. *Structural and Residual Stress Analysis by Nondestructive Methods.* Elsevier (1997).
[7] T.M. Holden, R.A. Holt, and A.P. Clarke. *Materials Science and Engineering A*, 246, 180–198 (1998).
[8] B. Clausen, T. Lorentzen, M.A.M. Bourke, and M.R. Daymond. *Materials Science and Engineering A*, 259, 17–24 (1999).
[9] M.R. Daymond, M.A.M. Bourke, R.B. Von Dreele, B. Clausen, and T. Lorentzen. *Journal of Applied Physics*, 82(4), 1554–1562 (1997).
[10] J.W.L. Pang, T.M. Holden, and T.E. Mason. *Acta Materialia*, 46(5), 1503–1518 (1998).
[11] J.W.L. Pang, T.M. Holden, and T.E. Mason. *Journal of Strain Analysis*, 33(5), 373–383 (1998).
[12] T.M. Holden, A.P. Clarke, and R.A. Holt. *Metallurgical and Materials Transactions A*, 28A, 2565–2576 (1997).
[13] H.J. Stone, T.M. Holden, and R.C. Reed. *Acta Materialia*, 47(17), 4435–4448 (1999).
[14] D. Dye, S.M. Roberts, and R.C. Reed. In *Proceedings of the Sixth International Conference on Residual Stresses ICRS-6*, p1317–1324. Institute of Materials, London, UK (2000).
[15] D. Dye, S.M. Roberts, P.J. Withers, and R.C. Reed. *Journal of Strain Analysis*, 35(4), 247–259 (2000).
[16] M.V.R.S. Jensen, D. Dye, K.E. James, A.M. Korsunsky, S.M. Roberts, and R.C. Reed. *Metallurgical and Materials Transactions A* (2002) *in press.*
[17] H.J. Stone, P.J. Withers, T.M. Holden, S.M. Roberts, and R.C. Reed. *Metallurgical and Materials Transactions A*, 30A, 1797–1807 (1999).
[18] H. J. Stone. *The Characterisation and Modelling of Electron Beam Welding.* PhD. thesis, Cambridge University, U.K. (1999).
[19] M. R. Daymond, C. N. Tomé, and M. A. M. Bourke. *Acta Materialia*, 48, 553–564 (2000).
[20] T. W. Eagar. In S. A. David and J. M. Vitek, editors, *Proceedings of the Conference on Recent Trends in Welding Science and Technology, Gattlinburg, Tennessee*, p341–346, ASM Int'l, OH, USA (1989).
[21] ASTM Standard E837. Determining residual stresses by the hole-drilling strain gauge method. ASTM, USA (1989).
[22] G. E. Dieter. *Mechanical Metallurgy.* McGraw-Hill Book Company (1988).